nature communications

Article

https://doi.org/10.1038/s41467-025-58666-w

The role of pyruvate dehydrogenase in the lifespan determination of *daphnids*

Received: 5 July 2024

Accepted: 28 March 2025

Published online: 05 April 2025

Check for updates

Wenkai Chen[1,2], Xueying Xu[1,2], Zhidan Zeng[1], Mingsen Zhou[1], Jiying Chen[1], Guangfu Hu[1], Anfu Shen[1], Dapeng Li[1] & Liu Xiangjiang[1]

The general association between longevity and energy metabolism has been well-documented for some time, yet the specific metabolic processes that regulate longevity remain largely unexplored. In contrast to the common active swimming *daphnids* (e.g., *Daphnia sinensis*), *Simocephalus vetulus* is notable for being sedentary and having a lower metabolic rate, yet it has a longer lifespan than *D. sinensis*. In this study, metabolomic analysis and drug validation experiments are employed to demonstrate that the lower pyruvate dehydrogenase (PDH) activity reduces the locomotor performance of *S. vetulus* and to identify PDH activity as a regulator of the lifespan of *daphnids*. Inhibition of PDH activity in *daphnids* by CPI-613 attenuates its ATP supply and locomotor performance but significantly induces longevity. The study also determines that the invertebrate neurotransmitter octopamine and temperature have a significant impact on PDH activity and modulate *daphnids* lifespan. And when the effects of temperature and octopamine on PDH activity are counteracted by inhibitors or agonists, the impact on lifespan becomes ineffective. These results support an important role for PDH in lifespan regulation and locomotor performance in *daphnids* and provide insights into the metabolic regulation of lifespan.

Water flea, the most commonly used model organism in ecological and toxicological studies, is emerging as a model organism for lifespan studies due to its short life cycle, easily controlled growth conditions, solitary reproduction, clear genetic background (multi-genome sequencing), and abundant genetic resources[1–5]. Almost all *daphnids* live a planktonic life throughout their lives, which largely depends on their grazing patterns and avoidance of enemies. However, *Simocephalus vetulus* exhibits a markedly different behavioral pattern in this regard. For the majority of its life history, *S. vetulus* was essentially attached to water plants. It even evolved a unique limb feature in which the outermost swimming setae of its second antennae were curved in the form of hooks to facilitate stable hooking to water plants. *Daphnia sinensis*, which inhabited the same habitat as *S. vetulus*, were selected as a representative species of common *daphnids* for comparison with *S. vetulus*. A noteworthy observation was that the sedentary *S. vetulus* exhibited a lower metabolic rate than the active *D. sinensis*, and also demonstrated a greater longevity at a similar body size. The relationship between energy metabolism, exercise and longevity has long been of interest[6]. Differences in locomotor habits, metabolism, and longevity between *S. vetulus* and *D. sinensis* have led to their consideration as good material for studying the relationship between locomotion, metabolism, and longevity.

The influence of metabolism on lifespan is a topic that has been extensively studied in the field of lifespan research. A substantial body of research has demonstrated a strong correlation between lifespan and metabolic rate. In *Caenorhabditis elegans*, mutants with increased longevity exhibit a reduction in metabolic rate. Once these mutants are returned to their original lifespan using genetic inhibitors, their metabolic rates also return to normal levels[7]. Furthermore, it has been demonstrated that environmental conditions which reduce the metabolic rate of *C. elegans* also result in an extension of their lifespan. Thus, Van and Ward concluded that the extension of *C. elegans* lifespan

[1]College of Fisheries, Huazhong Agricultural University, Wuhan 430070, China. [2]These authors contributed equally: Wenkai Chen, Xueying Xu.
e-mail: liuxiangjiang@mail.hzau.edu.cn

may not be a consequence of altered genetic pathways, but rather a consequence of their reduced metabolic rate. Furthermore, the effect of glucose metabolism on longevity seems to require more attention in exploring the relationship between longevity and energy metabolism[8–12]. An increase in glucose intake is associated with a reduction in lifespan, whereas impaired glucose metabolism is linked to an extension of lifespans[8,9]. It has been demonstrated that sustained glycolysis tends to accelerate the ageing process, and that lifespan interventions such as calorie restriction can extend lifespan by reducing the metabolic flux of glycolysis[13]. This result has also been validated in yeast experiments[14]. This hypothesis is further supported by the results of RNAi studies of two glycolytic genes in *C. elegans*[10,11].

Lionaki et al. demonstrated that reduced mitochondrial protein inputs extend lifespan in *C. elegans* by facilitating metabolic shifts in the conversion of glucose to serine, and that the essence of this action lies in the fact that mitochondrial dysfunction limits the oxidative phosphorylation process[15]. When mitochondrial dysfunction occurs, glycolysis increases to compensate for the decrease in the amount of aerobically produced ATP, but does not counteract the lifespan extension for *C. elegans*. This suggests that the role of glycolysis on lifespan lies not at its own level, but more likely in a limiting effect on downstream oxidative phosphorylation processes. It has long been reported that mild inhibition of mitochondrial respiration extends the lifespan of many organisms[16]. Metabolic data from a number of small rodent long-lived species supports this view. Both the naked mole rat (*Heterocephalus glaber*) and the Damaraland mole rat (*Fukomys damarensis*), which exhibit extraordinary longevity compared to their counterparts, have low basal metabolic rates and both rely more on glycolysis than oxidative phosphorylation[17]. Energy metabolism not only has a major impact on the lifespan of an organism, but also has a profound effect on its motility and athletic performance. Given the observed differences in locomotor behavior and longevity between *S. vetulus* and *D. sinensis*, it is plausible to suggest that energy metabolism plays a significant role in the poor locomotor performance and longevity of *S. vetulus*.

The present study has demonstrated an inverse correlation between pyruvate dehydrogenase complex (PDH) activity and lifespan. The use of metabolomic, behavioral and lifespan assays in *S. vetulus* and *D. sinensis* revealed that decreased PDH activity not only limits *Daphnids* locomotor performance by regulating glucose metabolism for energy supply, but also regulates energy metabolism rates and extends *Daphnids* lifespan. This provides insights into the intrinsic link between metabolism and lifespan, helps us to understand the mechanism of life aging and longevity more deeply, and also provides multiple perspectives and ideas for human anti-aging research.

Results

Sedentary *S. vetulus* lives longer than active *D. sinensis*

Both *S. vetulus* and *D. sinensis* were obtained and established as clone lines from the South Lake in Wuhan. The initial observation that led to the study of these two species was the observation of divergent locomotor habits, thus prompting an examination of the morphological differences in their swimming limbs. The outermost swimming setae of the second appendage of sedentary *S. vetulus* are curved and hooked at the end. These setae are hooked at the distal end, which anchors *S. vetulus* to the surface of the water plants (Fig. 1a). In contrast, the outermost swimming setae of the second appendage of active *D. sinensis* are covered with fine hairs, a feature that enhances its swimming ability (Fig. 1a). The genome sequence and assembly of *D. sinensis* was previously completed[5]. In order to achieve a more profound comprehension of the evolutionary relationships and divergence times of *S. vetulus* and *D. sinensis*, we undertook the sequencing and assembly of the genome of *S. vetulus*. Third-generation genome sequencing of *S. vetulus* yielded a 144.98 Mb genome with an N50 of 1.34 M and a GC content of approximately 39.50% (Fig. 1b). The genomes of *S. vetulus* and *D. sinensis* were compared at the chromosomal level using Minimap2 (version 2-2.26, parameters: -x asm5), and covariance circles were plotted using Circos (version 0.69-6) (Fig. 1c). The genomic chromosomes of *S. vetulus* and *D. sinensis* display a significant number of co-linear segments, thereby confirming the close affinity and high chromosomal synteny of the two species. With regard to the divergence time, *S. vetulus* was separated from other cladocerans as early as approximately 237.9 (17.2-308.6) million years ago (Supplementary Fig. 1).

Further, the life-history characteristics of *S. vetulus* and *D. sinensis* were compared. The life history observations of the two cladocerans revealed that the average lifespan of *S. vetulus* is 53.4 days, while the average lifespan of *D. sinensis* is only 44.4 days (Fig. 1d). Moreover, *S. vetulus* exhibited a younger age at first reproduction and a smaller body length at first spawning compared to *D. sinensis* (Fig. 1e and f). *S. vetulus* exhibited a longer inter-clutch period than *D. sinensis*, while also having smaller brood size (litters) and total reproductive capacity (lifetime litters) compared to *D. sinensis* (Fig. 1g, h and i). In general, fast development, early sexual maturation leading to early reproductive effort, as well as production of many offspring, have been linked to shorter lifespans[18]. *D. sinensis* with greater total reproductive capacity and shorter inter-clutch period had significantly lower longevity than *S. vetulus*.

In order to visually compare the differences in locomotor habits between *S. vetulus* and *D. sinensis*, an investigation was conducted into the swimming behavior and locomotion-related physiological indicators. Behaviorally, the frequency of hopping and locomotor activity were found to be significantly lower in *S. vetulus* compared to *D. sinensis* (Fig. 1j and k). The three-minute video observation revealed that *S. vetulus* exhibited a high degree of immobility, remaining stationary for an average of 92.7% of the observation period. In contrast, *D. sinensis* swims at almost all the time, averaging only about 2.3% of the observation period without swimming (Fig. 1l). A high level of exercise is often accompanied by a high metabolic rate, which is reflected in the demand for food and oxygen. Research has demonstrated that *D. sinensis* exhibits a markedly higher feeding rate and oxygen consumption than *S. vetulus* (Fig. 1m and n). Overall, the behavioral and physiological characteristics observed in both species of *daphnids* were consistent with their respective locomotor habits.

Ability rather than willingness to exercise leads to differences in locomotor choice

To further understand the reasons for the different locomotor choices of the two species, forced exercise experiments were conducted on both *S. vetulus* and *D. sinensis*. Petri dishes containing all the *daphnids* were placed on a fixed-rail shaker. The fluctuations in the water column and the smooth surface of the petri dishes forced *S. vetulus* and *D. sinensis* to swim. Although the natural water body in which *S. vetulus* lives is also non-stationary, a blade of watercress was placed in a petri dish with *S. vetulus* to eliminate the influence of stress on the results. The good condition of *S. vetulus* hooked itself on the surface of the watercress leaf in the same fluctuating water body indicates that water fluctuations in the forced-motion experiment do not cause stress to *S. vetulus*. During the sixth hour of the experiment, over 50% of swimming *S. vetulus* exhibited difficulty swimming in the water and sank to the bottom of the petri dish (Fig. 2a and b). In contrast, *D. sinensis* continued to swim normally. After cessation of disturbance to the water column, *S. vetulus* showed gradual recovery. ATP levels and lactate levels were measured in both *S. vetulus* and *D. sinensis* after 6 hours of forced exercise. ATP concentrations decreased significantly in both *S. vetulus* and *D. sinensis*, but the decrease was greater in *S. vetulus* (56.9% in *S. vetulus*, 22.9% in *D. sinensis*) (Fig. 2c). Lactate levels were also significantly increased in *S. vetulus* but not in *D. sinensis* (Fig. 2d). These results demonstrate the inferior ATP supply and aerobic metabolism of *S. vetulus* compared to *D. sinensis*.

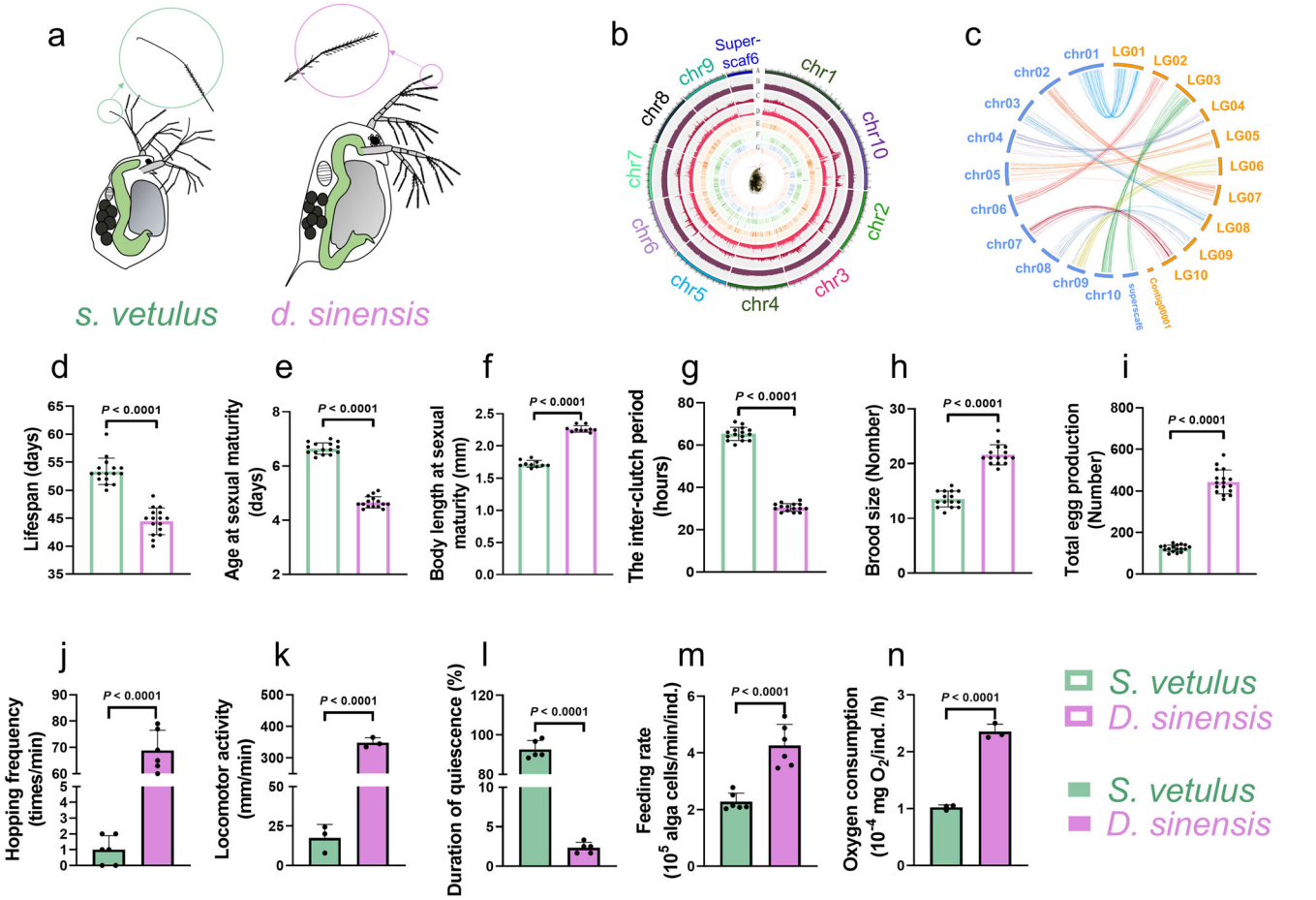

Fig. 1 | Comparison of the genomic, life history, and behavioral characteristics of *S. vetulus* and *D. sinensis*. **a** Diagrams of parthenogenic female *S. vetulus* and *D. sinensis*. **b** Genome circle diagram of *S. vetulus*. (A, Genomic information; B, GC content distribution; C, Depth distribution of second-generation reads; D, Depth distribution of third-generation reads; E, Outer circle for pure SNP distribution, inner circle for heterozygous SNP distribution; F, Pure InDel distribution in the outer circle, heterozygous InDel distribution in the inner circle; G, Distribution of genes on the genome for complete comparison BUSCO, single-copy BUSCO in blue, duplicated BUSCO in red). **c** Genomic covariance analysis of *S. vetulus* and *D. sinensis*. The letters "chr" and "LG" represent the chromosomes of *S. vetulus* and *D. sinensis*, respectively. **d** The lifespans of *S. vetulus* and *D. sinensis* ($n = 16$). **e** Age of *S. vetulus* and *D. sinensis* at sexual maturity ($n = 15$). **f** Body length of *S. vetulus* and *D. sinensis* at sexual maturity ($n = 10$). **g** The inter-clutch period of *S. vetulus* and *D. sinensis* (N = 15). **h** Brood size, average number of offspring per litter of *S. vetulus* and *D. sinensis* ($n = 15$). **i** Total number of offspring produced throughout the life history ($n = 17$). **j** The frequency of hops for swimming of *S. vetulus* and *D. sinensis* ($N = 6$). **k** Locomotion per unit time in *S. vetulus* and *D. sinensis* ($N = 3$). **l** Duration of quiescence of *S. vetulus* and *D. sinensis* ($N = 5$). **m** Feeding rate of *S. vetulus* and *D. sinensis* ($N = 6$). **n** Oxygen consumption in *S. vetulus* and *D. sinensis* ($N = 3$). N, number of replicates; n, number of samples per replicate. **d**–**n** The raw data are presented as means ± SEM and were analyzed by unpaired two-tailed Student's t-test after normality and homogeneity of variance was confirmed. Source data are provided as a Source Data file.

Lower PDH activity limits locomotor activity and prolongs lifespan in *S. vetulus*

Forced exercise experiments demonstrated the inferior aerobic metabolism of *S. vetulus* relative to *D. sinensis*, so the two species were analyzed metabolically, and key metabolites of energy metabolism were compared. The metabolomic analysis of *S. vetulus* and *D. sinensis* revealed 153 differential metabolites (DMs) that were significantly enriched in the pathways related to glucose metabolism (Fig. 3a). The levels of pyruvate and lactate were found to be significantly higher in *S. vetulus* than in *D. sinensis*, while the levels of acetyl coenzyme A and ATP were found to be significantly lower in *S. vetulus* than in *D. sinensis* (Fig. 3b). Normally, pyruvate, the end product of glycolysis, is generated by pyruvate dehydrogenase (PDH) to produce acetyl coenzyme A, which enters the tricarboxylic acid cycle and ultimately generates ATP by oxidative phosphorylation to supply energy to the body. Once the pyruvate oxidative decarboxylation process is blocked, pyruvate accumulates in large quantities and is reversibly converted to lactate. Furthermore, the production of pyruvate oxidative decarboxylation products, acetyl coenzyme A and ATP, is also reduced. The pyruvate dehydrogenase complex (PDC) is responsible for the oxidative decarboxylation of pyruvate. The complex comprises three components: pyruvate dehydrogenase (E1), dihydrolipoamide acetyltransferase (E2), and dihydrolipoamide dehydrogenase (E3)[19]. The nucleic acid sequences of the pyruvate dehydrogenase complex E1, E2, and E3 from *S. vetulus* and *D. sinensis* were extracted from their respective genomes. Sequence analysis software and SWISS-MODEL were employed to facilitate the comparison of amino acid sequence and protein structures (Supplementary Fig. 2 and 3). The structure of the PDH α-subunit differs significantly between *S. vetulus* and *D. sinensis* (Supplementary Fig. 4). Furthermore, prediction of the interaction between pyruvate dehydrogenase and thiamine pyrophosphate using AlphaFold 3. The interaction prediction between PDH from *D. sinensis* and thiamine pyrophosphate yielded a higher ranking score compared to that from *S. vetulus*. (Fig. 3c). The results of metabolomics analysis and PDH sequence and structure analysis suggest that the pyruvate oxidative decarboxylation process in *S. vetulus* may be impaired (Fig. 3d).

Furthermore, CPI-613 (Devimistat, a PDH indirect inhibitor) and DCA (sodium dichloroacetate, a PDH indirect agonist) were utilized in

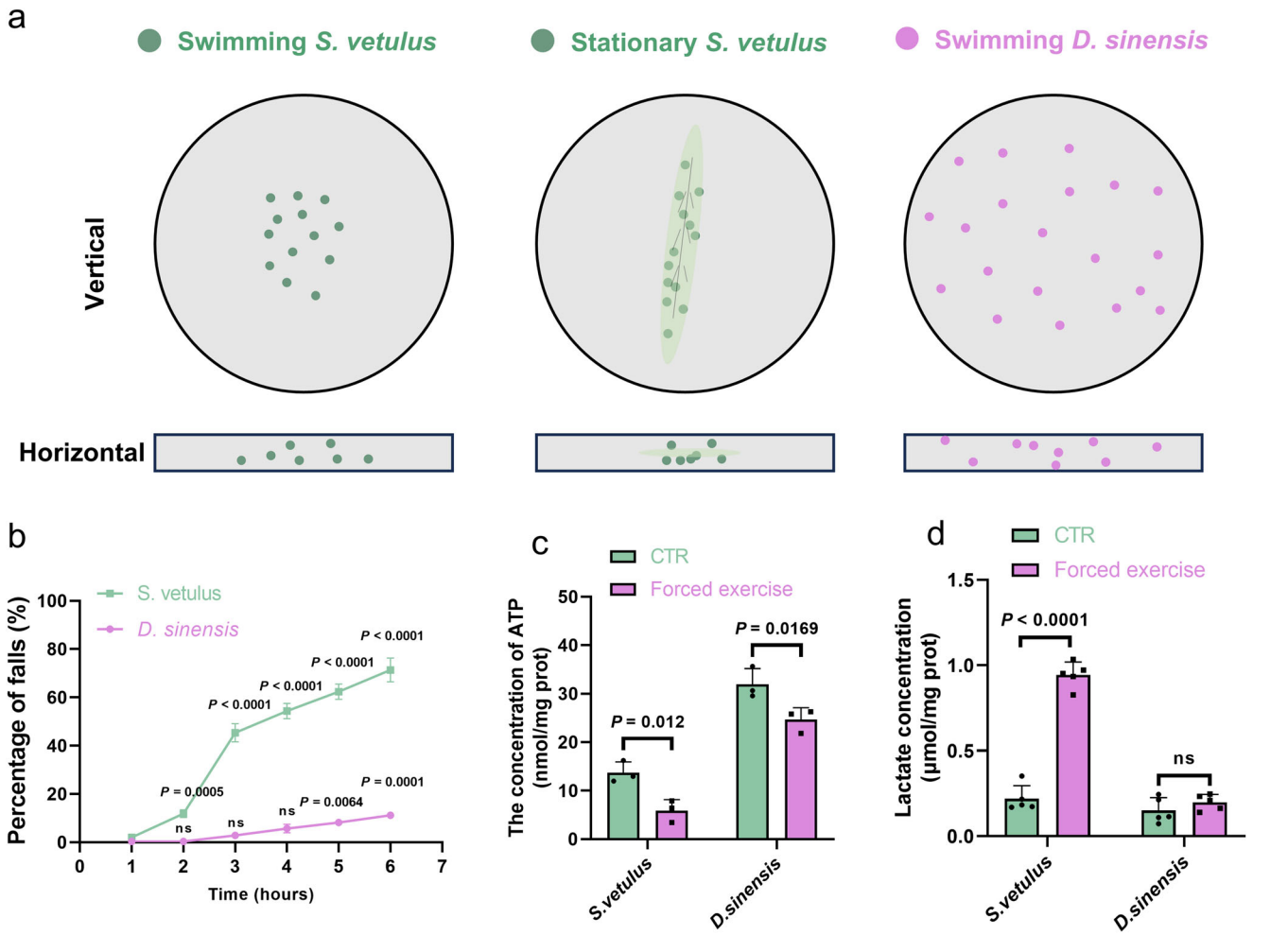

Fig. 2 | Locomotor ability, but not locomotor willingness, influences locomotor choice in *S. vetulus* and *D. sinensis*. **a** The horizontal and vertical distribution of *S. vetulus* and *D. sinensis* in petri dishes following six hours of the forced exercise experiment ($N = 3$). **b** The proportion of falls over time in the forced exercise experiments with *S. vetulus* and *D. sinensis* ($N = 3$, $n = 30$). Statistical significance was determined by two-way ANOVA with Tukey's multiple-comparisons test. **c** The ATP content of *S. vetulus* and *D. sinensis* after 6 hours of forced exercise ($N = 3$). Statistical significance was determined by two-way ANOVA with Sidak's multiple-comparisons test. **d** The lactate concentration of *S. vetulus* and *D. sinensis* after 6 hours of forced exercise ($N = 5$). Statistical significance was determined by two-way ANOVA with Sidak's multiple-comparisons test. All data are presented as means ± SEM. Source data are provided as a Source Data file.

the treatment of *S. vetulus* and *D. sinensis*[20–22]. Higher concentrations (≥10 μM) of the PDH inhibitor CPI-613 resulted in increased mortality rates at 24 h, 96 h, and 240 h in both species (Fig. 3e and f), and all concentrations of DCA used in the experiments did not result in the death of *daphnids*. DCA dose-dependently promoted PDH activities, and CPI-613 dose-dependently inhibited PDH activities over the concentration range tested (Fig. 3g and h). Subsequently, locomotor trajectories were recorded, and locomotor vigor was calculated for 10 μM DCA-treated *S. vetulus* for 24 h and 10 μM CPI-613-treated *D. sinensis* for 24 h. The results showed that 10 μM DCA significantly enhanced PDH activities in *S. vetulus*. 10 μM DCA significantly enhanced the locomotor vigor of *S. vetulus*, and 10 μM CPI-613 also promoted the locomotion of *D. sinensis* (Fig. 3i), and acetyl coenzyme A supplementation improves indirectly exercise performance and ATP production (Supplementary Fig. 4). The effects of DCA and CPI-613 on PDH activities were ultimately reflected in the ATP content (Fig. 3j and k).

In aquatic animal studies, standard metabolic rate (SMR) is usually measured using respirometry (measurement of oxygen consumption), and thus oxygen consumption is used as a reflection of the overall metabolic rate of *daphnids*[23,24]. The oxygen consumption of *D. sinensis* was found to be higher than that of *S. vetulus* under normal conditions. The agonistic and inhibitory effects of DCA and CPI-613 on PDH activities elevated the oxygen consumption of *S. vetulus* and decreased the oxygen consumption of *D. sinensis*, respectively (Fig. 3l). The relationship between metabolic rate and lifespan was further examined by quantifying the lifespan of *S. vetulus* and *D. sinensis* treated with DCA and CPI-613, respectively. The lifespan of *D. sinensis*, which originally exhibited a high metabolic rate, was found to be significantly extended after its metabolism was reduced by CPI-613 (Fig. 3m). In contrast, *S. vetulus*, which initially exhibited a lower metabolic rate, demonstrated an elevated metabolic rate and a significantly diminished lifespan following DCA treatment (Fig. 3n). Diminished reproductive capacity and decreased heart rate are considered important phenotypes of senescence in *daphnids*[2,25]. Statistics on reproductive capacity and heart rate on days 20 and 40 of both species showed that CPI-613 and DCA slowed and accelerated senescence in *daphnids*, respectively (Supplementary Fig. 5). To further validate the role of PDH in determining lifespan in *daphnids*, the *pdha* gene was knocked out in *D. sinensis* (Supplemental Video 1). Unfortunately, all *pdha* mutants died before 30 hours (Supplementary Fig. 6). None of the *pdha* of the individuals that continued to develop were mutated, and therefore adult homozygous mutants could not be obtained for lifespan studies. PDH activity not only appears to affect *daphnids* motility, a key valve for energy supply, but is likely to be involved in lifespan regulation by affecting metabolic rates.

https://doi.org/10.1038/s41467-025-58666-w

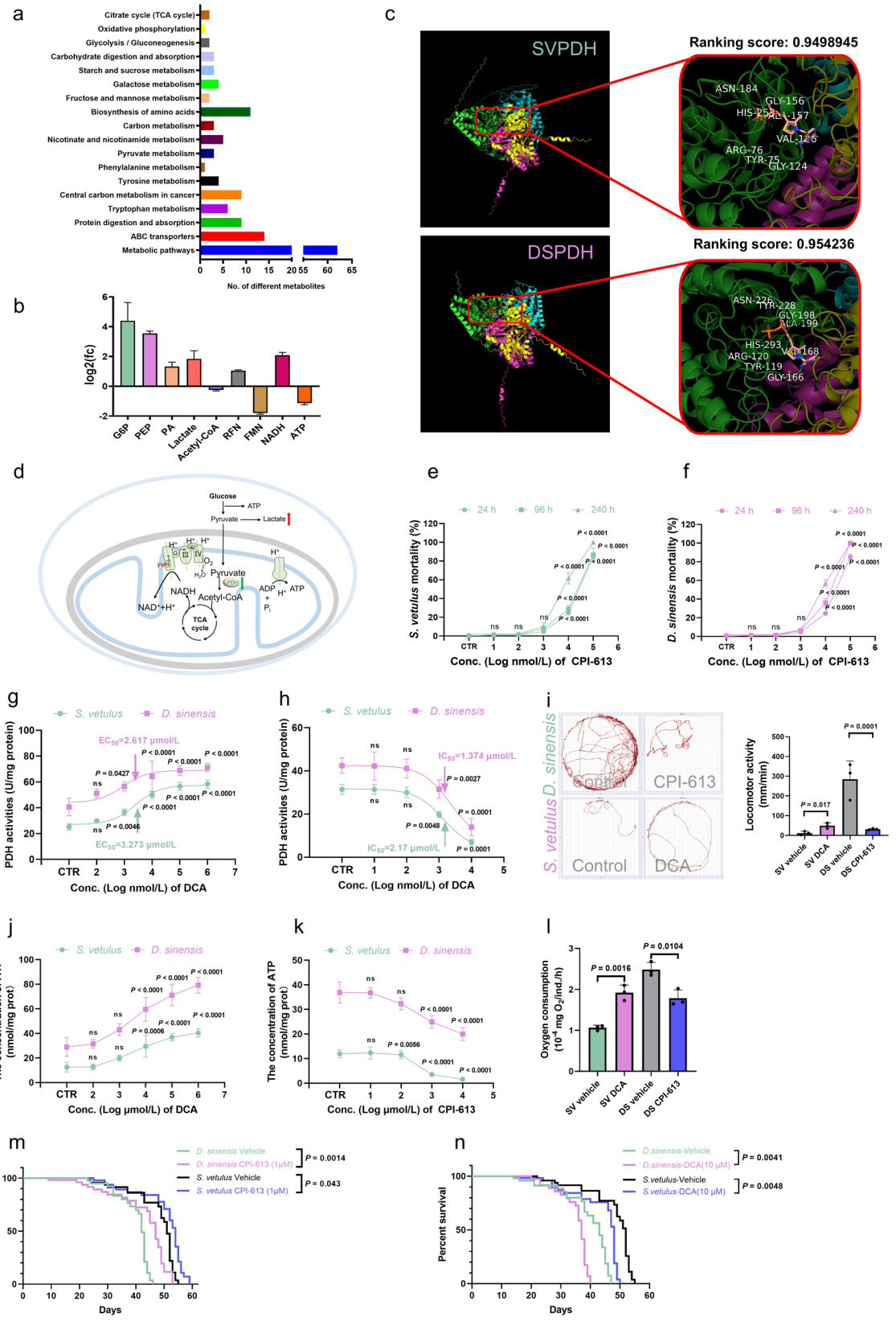

Octopamine enhances motility and shortens lifespan of *daphnids* by enhancing PDH activity

Octopamine is responsible for coordinating the transition from a resting state to a more active state in insects, and plays a significant role in the induction and maintenance of invertebrate locomotion[26]. Octopamine-deficient *Drosophila* have reduced physical activity and lower resting metabolic rate[26,27]. Octopamine levels were assayed in *S. vetulus* and *D. sinensis* due to the important role of octopamine in the regulation of locomotion and organismal metabolic rates in invertebrates. The enzyme-linked immunosorbent assay demonstrated that the octopamine levels in *S. vetulus* were markedly lower than those observed in *D. sinensis* (Fig. 4a). To ascertain whether octopamine

Fig. 3 | Impaired energy metabolism limits locomotion but extends longevity in *S. vetulus*. **a** KEGG pathway enrichment analysis of differential metabolites of *S. vetulus* and *D. sinensis*. **b** Differential metabolites related to glucose metabolism. **c** Binding site prediction and conformation simulation of pyruvate dehydrogenase (PDH) and thiamine pyrophosphate by AlphaFold 3. SVPDH, *S. vetulus* pyruvate dehydrogenase; DSPDH, *D. sinensis* pyruvate dehydrogenase; The two α subunits are labelled green and blue and the two β subunits are labelled red and yellow. **d** Schematic representation of glucose metabolism and oxidative phosphorylation. **e** The mortality of *S. vetulus* treated with gradient concentrations of CPI-613 ($N = 3$). **f** The mortality of *D. sinensis* treated with gradient concentrations of CPI-613 ($N = 3$). **g** The PDH activities of *S. vetulus* and *D. sinensis* treated with gradient concentrations of DCA ($N = 3$). **h** The PDH activities of *S. vetulus* and *D. sinensis* treated with gradient concentrations of CPI-613 ($N = 3$). **i** The exercise trajectories and locomotor activity of 10 μM CPI-613-treated *D. sinensis* and 10 μM DCA-treated *S. vetulus* ($N = 3$). **j** The ATP content of *S. vetulus* and *D. sinensis* treated with gradient concentrations of CPI-613 ($N = 6$). **k** The ATP content of *S. vetulus* and *D. sinensis* treated with gradient concentrations of DCA ($N = 6$). **l** The metabolic rate of 10 μM DCA-treated *S. vetulus* and 1 μM CPI-613-treated *D. sinensis* ($N = 3$). **m** The lifespan of CPI-613-treated *S. vetulus* and *D. sinensis* ($n = 30$). **n** The lifespan of DCA-treated *S. vetulus* and *D. sinensis* ($n = 30$). SV, *S. vetulus*. DS, *D. sinensis*. For (**e**–**i**), all data are presented as means ± SEM. Statistical significance was determined by two-way ANOVA with Dunnett's multiple-comparisons test (**e, f, j** and **k**), two-way ANOVA with Sidak's multiple-comparisons test (**g** and **h**), unpaired two-tailed Student's t-test (**i**) or Survival curve comparison with Gehan-Breslow-Wilcoxon test (**m** and **n**). Source data are provided as a Source Data file.

plays a role in the regulation of locomotion in *daphnids*, the locomotor activity and trajectory in octopamine-treated *S. vetulus* and *D. sinensis* were measured. The experimental results demonstrated that octopamine treatment could significantly induce locomotion in *S. vetulus* and *D. sinensis* in a dose-dependent manner (Fig. 4b). Furthermore, 1 μM octopamine has been demonstrated to stimulate PDH activity (Fig. 4c), increase ATP content (Fig. 4d) and enhance oxygen consumption (Fig. 4e) in both *S. vetulus* and *D. sinensis*. Given the enhancement of PDH activity by octopamine, we observed the lifespan of *S. vetulus* and *D. sinensis* under long-term treatment with 1 μM octopamine. As anticipated, 1 μM octopamine markedly reduced the lifespan of *S. vetulus* and *D. sinensis* (Fig. 4f). To determine whether octopamine affects locomotor performance and longevity through PDH rather than other pathways, octopamine and the PDH inhibitor CPI-613 were co-treated in both species. 1 μM CPI-613 was used to counteract the enhancing effect of octopamine on PDH activity (Fig. 4g), and octopamine was no longer able to shorten lifespan in both species (Fig. 4h). These results provide further support for the involvement of octopamine in the regulation of life span by influencing PDH activity.

PDH activity is also involved in the regulation of *daphnids* lifespan by temperature

It is evident that temperature is a crucial factor that influences the lifespan of *daphnids*[28]. Lifespan analysis experiments have corroborated the correlation between lifespan and temperature in *S. vetulus* and *D. sinensis*. Both *S. vetulus* (Fig. 5a) and D. *sinensis* (Fig. 5 b) exhibited a significantly shorter lifespan in high-temperature (35 °C) environments and a prolonged lifespan in low-temperature (15 °C) environments. Furthermore, Octopamine levels in *S. vetulus* and *D. sinensis* exhibited a positive correlation with increasing temperature (Fig. 5c), which is in line with the trend of octopamine and temperature effects on lifespan. It is likely that these potential lifespan regulators act synergistically in organisms, particularly in their effects on metabolism. The detection of PDH activity at varying temperatures in both *S. vetulus* (Fig. 5d) and D. *sinensis* (Fig. 5e) revealed an increase of PDH activity with rising temperature. The same applies to the ATP content (Fig. 5f) and their locomotion (Fig. 5g). Similar to octopamine, the longevity effect was also no longer significant after the inhibition of PDH activity by low temperature was rescued by a PDH agonist (10 μM DCA) (Fig. 5 h and i).The results of this study support the idea that PDH activity plays an important role in the regulation of locomotor performance and lifespan in *S. vetulus* and *D. sinensis*, and that PDH inhibitors and agonists, temperature, and octopamine all affect locomotor performance and lifespan in both *S. vetulus* and *D. sinensis* through modulation of PDH activity (Fig. 5j).

Discussion

The present study found that the lower PDH activity lowered the locomotor ability and athletic performance of *S. vetulus*, while elevated PDH activity was able to confer an enhancement of *daphnids* locomotor ability at the cost of a shorter lifespan. Previous studies on PDH have focused on its role in areas such as glucose-lipid metabolism, cancer therapy and insulin resistance/diabetes treatment[29–32]. Although the pivotal role of PDH in energy metabolism is well established, few studies have investigated the effects of PDH on energy metabolism with the aim of intervening in lifespan. The present study demonstrates that elevated PDH activity promotes oxidative phosphorylation (ATP synthesis) and oxygen consumption, yet it also shortens lifespan and enhances ATP availability for *daphnids* motility. This not only implies the possible discovery of a potential lifespan-modulating target but also suggests that drugs that target or indirectly modulate PDH in the clinic pose a pro-aging or short-life risk to patients.

The PDC is present in all organisms except viruses and is a fundamental component of energy metabolism in both prokaryotes and eukaryotes[33]. A reduction in PDH activity results in a physiological disorder known as pyruvate dehydrogenase complex deficiency (PDCD)[34,35]. Patients with PDCD exhibit reduced PDH activity in their cells, and typical symptoms include lactic acidosis, elevated levels of pyruvate, paroxysmal exercise-induced dyskinesia, and metabolic ataxia[34]. The elevated lactate and pyruvate levels observed in *S. vetulus* in this study are consistent with the typical symptoms of PDCD as described in the literature. The results of subsequent enzyme activity assay experiments confirmed the lower PDH activity of *S. vetulus* compared to *D. sinensis*. In human patients, PDCD is frequently attributed to mutations in the components that comprise the PDC[36]. PDH is the rate-limiting enzyme of the pyruvate dehydrogenase complex (PDHC), a tetramer composed of two PDH α subunits and two PDH β subunits. One of the most prevalent mutation types is mutations in the PDHα subunit, which are predominantly missense and code-shift mutations[37]. These mutations affect the binding of E1α to thiamin pyrophosphate cofactors, the formation of heterotetramers, and the ability to correctly target and translocate into mitochondria[34]. Thanks to the rapid development of artificial intelligence in structural biology, AlphaFold 3 was developed and proved to be accurate in predicting protein-small molecule interactions[38]. We predicted the interaction between PDH proteins and thiamine pyrophosphate in both species. The lower docking scores for the PDH protein-thiamine pyrophosphate interactions of *S. vetulus* support that changes in the amino acid sequence and protein structure of the *S. vetulus* PDH α-subunit may be the cause of the reduced activity of *S. vetulus* PDH. Thus, when *S. vetulus* was forced to exercise, the lower PDH activity resulted in a large accumulation of lactate and a significant deficit in ATP supply. However, further experimental validation is needed to confirm these predictions and fully understand the functional consequences. *S. vetulus* might be considered as a PDCD taxon in the *daphnids*. However, in contrast to the high mortality rate observed among human patients[34], *S. vetulus* is able to survive in nature as an intact population. This is likely to be related to the complex genesis of PDCD and the unique lifestyle of *S. vetulus*. Changes in PDH activity in human patients with PDCD caused by E1 mutations tend to be variably significant, ranging from approximately 10% to 60% of those in healthy

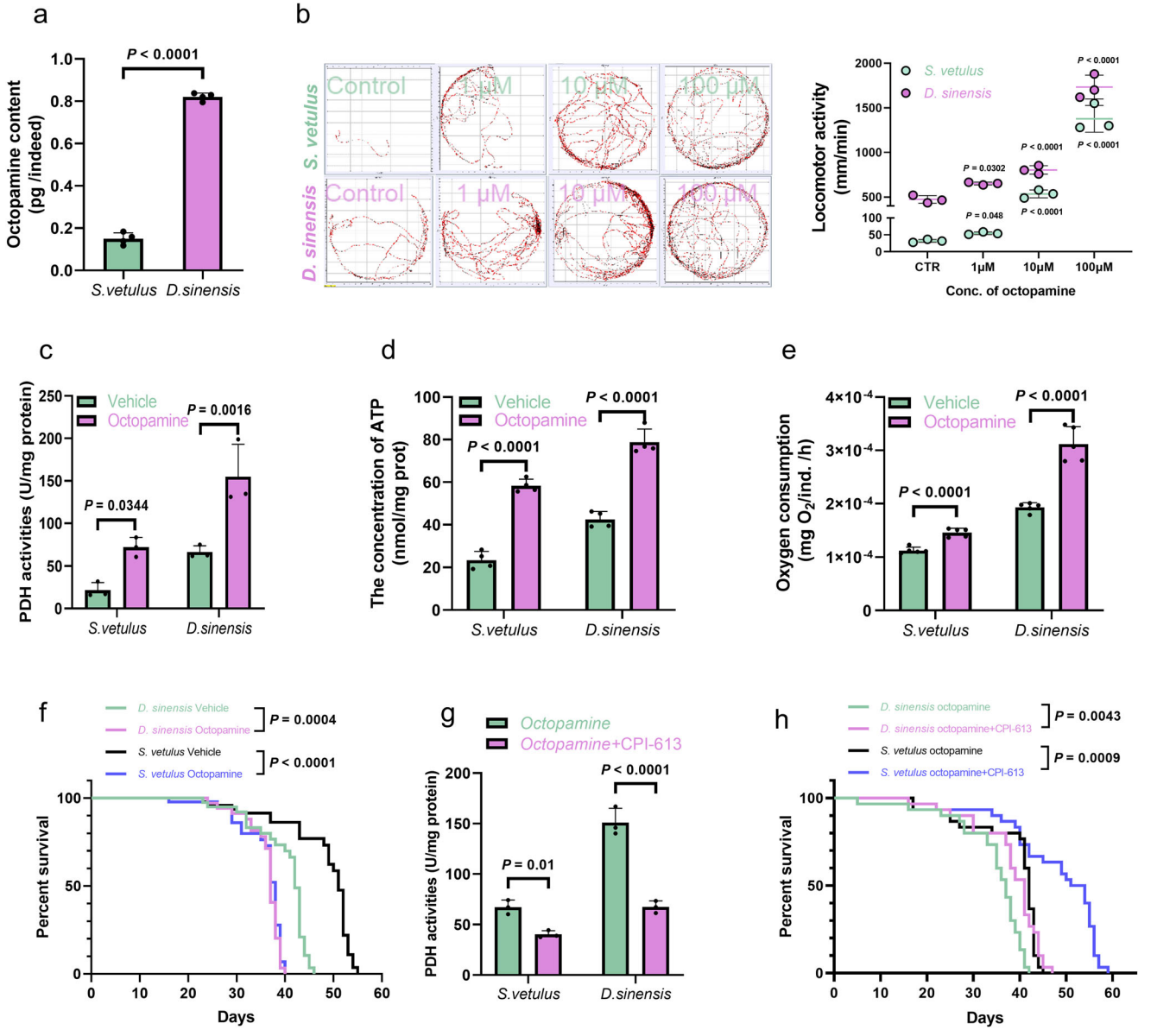

Fig. 4 | Octopamine could enhance exercise and metabolism, but impairs longevity. a The octopamine content of *S. vetulus* and *D. sinensis*($N = 3$). **b** The exercise trajectories of *D. sinensis* and *S. vetulus* treated with 1 μM, 10 μM and 100 μM octopamine (N = 3); The locomotor activity of *D. sinensis* and *S. vetulus* was measured in a 10 μM octopamine treatment. **c** PDH activity of *D. sinensis* and *S. vetulus* treated with 10 μM octopamine ($N = 3$). **d** ATP content of *D. sinensis* and *S. vetulus* treated with 10 μM octopamine ($N = 4$). **e** Metabolic rate of *D. sinensis* and *S. vetulus* treated with 10 μM octopamine ($N = 5$). **f** The lifespan of 10 μM octopamine-treated *S. vetulus* and *D. sinensis* ($n = 30$). **g** The PDH activity in *S. vetulus* and *D. sinensis* co-treated with 10 μM CPI-613 and 10 μM octopamine ($N = 3$). **h** The lifespan of 10 μM CPI-613 and 10 μM octopamine-treated *S. vetulus* and *D. sinensis* ($n = 30$). For (**a**–**e** and **g**), all data are presented as means ± SEM. Statistical significance was determined by unpaired two-tailed Student's t-test (**a**), two-way ANOVA with Sidak's multiple-comparisons test (**b, c, d, e** and **g**) or Survival curve comparison with Gehan-Breslow-Wilcoxon test (**f** and **h**). Source data are provided as a Source Data file.

individuals[34]. *S. vetulus* has only 30% to 40% of the PDH activity of *D. sinensis*, but is still partially functional. Apparently, the lower PDH activity is not sufficient to allow *S. vetulus* to exhibit the same level of free-swimming behavior as *D. sinensis*. However, the persistence of residual PDH activity ensures that glycolytic and oxidative phosphorylation processes are still functioning at low levels in resting *S. vetulus* to sustain life[36].

To date, there has been substantial experimental evidence to suggest that energy metabolism has a positive regulatory effect on lifespan[39–42]. Nevertheless, the molecular mechanisms by which energy metabolism regulates lifespan remain poorly understood. For a considerable period, the prevailing view has been that higher energy metabolism rates are associated with shorter lifespans, and vice versa. The findings of the present study indicate that an increasing in the metabolic rate of *daphnids* will result in a significantly reduction in lifespan. It is evident that this pattern is not exclusive to model organisms employed in longevity studies. A recent sex-specific Mendelian randomization survey in human subjects further supports this view and suggests that higher basal metabolic rates may shorten lifespan[39]. Furthermore, our findings indicate that the metabolic rate of *daphnids* is significantly influenced by glucose metabolic processes. A glucose-rich diet has been demonstrated to reduce lifespan in *C. elegans* by influencing the activity of longevity-promoting proteins, suggesting that glucose toxicity may be a contributing factor. This is often associated with increased mitochondrial respiration and oxidative stress[43]. The free radical theory of ageing postulates that reactive

https://doi.org/10.1038/s41467-025-58666-w

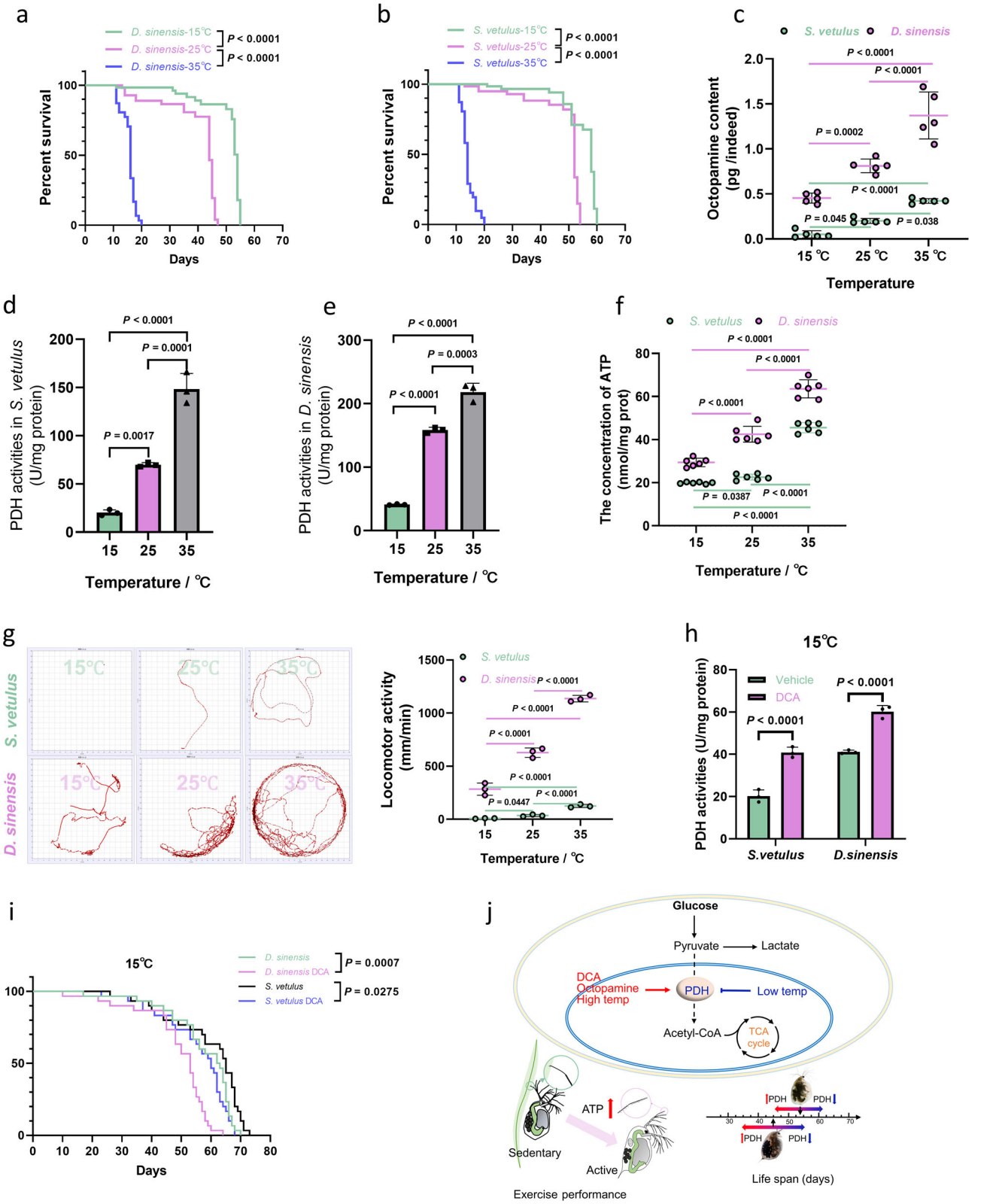

Fig. 5 | Low temperature extends *Daphnids* lifespan by inhibiting PDH activity. **a** The lifespan of *S. vetulus* at 15 °C, 25 °C and 35 °C ($n = 30$). **b** The lifespan of *D. sinensis* at 15 °C, 25 °C and 35 °C ($n = 30$). **c** The octopamine content of *S. vetulus* and *D. sinensis* at 15 °C, 25 °C and 35 °C ($N = 5$). **d** The PDH activity of *S. vetulus* at 15 °C, 25 °C and 35 °C ($N = 3$). **e** The PDH activity of *D. sinensis* at 15 °C, 25 °C and 35 °C ($N = 3$). **f** The ATP content of *S. vetulus* and *D. sinensis* at 15 °C, 25 °C and 35 °C ($N = 6$). **g** The exercise trajectories and locomotor activity of *S. vetulus* and *D. sinensis* at 15 °C, 25 °C and 35 °C ($N = 3$). **h** The PDH activity of CPI-613-treated *S. vetulus* and *D. sinensis* at 15 °C ($N = 3$). **i** The lifespan of CPI-613-treated *S. vetulus* and *D. sinensis* at 15 °C ($n = 30$). **j** PDH is involved in regulating motor performance and longevity in *Daphnia*. For (**c**–**h**), all data are presented as means ± SEM. Statistical significance was determined by Survival curve comparison with Gehan-Breslow-Wilcoxon test (**a, b** and **i**), two-way ANOVA with Sidak's multiple-comparisons test (**c, f, g** and **h**) or one-way ANOVA conducted with Tukey's multiple comparisons test (**d** and **e**). Source data are provided as a Source Data file.

oxygen species (ROS) are responsible for the oxidative damage that occurs in organisms, which in turn leads to the process of ageing. Mitochondria are the main ROS producers in organisms, with the respiratory chain serving as the site of electron transfer, resulting in the generation of superoxide anion[44]. In their study, Lionaki et al. demonstrated that the effects of a shortened lifespan resulting from diets high in glucose could be mitigated by inhibiting mitochondrial protein input[15]. Inhibition of mitochondrial protein input result in mitochondrial dysfunction, which in turn limits the capacity for mitochondrial oxidative phosphorylation, thereby prolonging the lifespan of *C. elegans*[15]. In the present study, we found that inhibition of PDH activity similarly also extends lifespan. Inhibition of PDH activity would be directly reflected in the downstream mitochondrial respiratory process, with reduced oxygen consumption and ATP production in *daphnids*. And the life-extending effect of mild inhibition of mitochondrial respiration has been demonstrated in a variety of organisms, including yeast, worms, flies, and mice[16]. Overall, this study provides a potential target for lifespan regulation, where PDH activity will influence lifespan through its effects on metabolic rate and downstream mitochondrial respiration.

In addition to the lifespan-regulating role of PDH activity, this study identified several modulators of PDH activity, including octopamine and temperature. Octopamine is a tyrosine-derived biogenic amine that has been reported to be involved in the regulation of energy homeostasis and the initiation of locomotion in invertebrates[26]. In *Drosophila*, octopamine regulates flight behavior (the most energy-intensive form of locomotion in insects) at several levels, in particular playing an important role in the initiation and duration of flight[45]. In this study, we found that octopamine levels were more than four times higher in *D. sinensis* than in *S. vetulus*. Exogenous octopamine was able to enhance locomotion in *S. vetulus*, and this enhancement was based on the mobilization of total metabolic levels in *S. vetulus*. Octopamine increased PDH activity, metabolic rate (oxygen consumption rate) and ATP production in *S. vetulus*. The enhancement of *S. vetulus* exercise performance by octopamine was based not only on increased willingness to exercise, but also on increased energy availability. In addition to enhancing glucose metabolism, octopamine is also thought to promote fat utilization, with both fasting and starvation capable of inducing octopamine release[46,47]. Octopamine-deficient *Drosophila melanogaster* exhibit an obese phenotype, and studies in grasshoppers and crickets have demonstrated the direct activation of fatty acid oxidation and carbohydrate release by octopamine[26]. Long-term treatment with octopamine also significantly shortened the lifespan of *daphnids*, which may be attributed to its PDH activating effects and acceleration of energy metabolism rates.

Temperature, another factor affecting locomotor performance and lifespan in *S. vetulus*, was also found to correlate with octopamine release and PDH activity. The traditional view of the effects of temperature on enzyme activity, metabolism and lifespan of organisms is based on purely thermodynamic effects, but recent studies have increasingly emphasized the important role of genetic regulation in that[48,49]. In the present study, we found that the effects of temperature on PDH activity and lifespan are not based on purely thermodynamic effects, and that octopamine is significantly increased in synthesis and release by temperature, and that this effect is realized in both *S. vetulus* and *D. sinensis*. And the inhibition of low temperature on PDH activity in both species was resecured by DCA treatment, and the extension of their lifespan by low temperature was counteracted. These results support a critical role for PDH activity in temperature-to-lifetime modulation, rather than a simple thermodynamic effect. Octopamine is a neuroactive substance that is the invertebrate equivalent of adrenergic signaling compounds[27]. One possible regulatory pathway is that stimulation of cladocerans by the external environment first elicits a response in octopamine levels, which mobilizes the body's glycolipid metabolism and provides energy security for the organism. Indeed, our results are biased in favor of octopamine as a stress-responsive compound in dendrobatids.

The present study demonstrates that proper inhibition (not deletion) of PDH in *S. vetulus* and *D. sinensis* reduces metabolism (level of oxygen consumption) and contributes to longevity. As an additional consequence of PDH inhibition, locomotor performance and exercise performance subsequently deteriorated. However, there is a consensus in the human world is that life is all about exercise. The longevity benefits of exercise have been widely reported. Among other mechanisms mediating protective effects of exercise, periodic exercise, while increasing heart rate during exercise, appears to reduce resting heart rate[50], which in some respects may be a proxy for metabolic rate and which also inversely correlates with lifespan in terrestrial mammals. Although metabolic rate (e.g., as indicated by heart rate) increases during exercise, the net effect of exercise is to reduce overall heart rate (after cessation of exercise) and thus, plausibly, total net metabolism. Athletes tend to have lower resting heart rates and lower resting metabolic rates as well as longer life expectancies compared to the general population. And a statistically significant association between increased resting heart rate and mortality risk has been reported[51]. Among *daphnids*, more physically active *D. sinensis* had shorter lifespans, which seems to contradict the common understanding that exercise is beneficial for lowering total net metabolism and longevity. But the effects of exercise on metabolic rate must be considered separately as the immediate effects (metabolic rate tends to increase during exercise) and the long-term effects (total net metabolism decreases due to the exercise of the body's aerobic respiratory capacity). In fact, it should not be overlooked that as a zooplankton, *D. sinensis*, swims throughout its life, which is very different from the periodic exercise performed by athletes. Exercise in *D. sinensis* corresponds to a non-stop immediate effect resulting in a persistent high metabolic rate, and therefore *D. sinensis* as an "exercise enthusiast" does not enjoy the life-extending benefits of exercise.

Methods

Animal culture and sample collection

The clones of *S. vetulus* (LN2017 strain) and *D. sinensis* (WSL strain) were originally isolated from the South Lake (Wuhan, Hubei, China), and the clone lines were initiated from a single parthenogenetic female and cultured for years in the laboratory. The *daphnids* (*Daphnia sinensis* and *Simocephalus vetulus*) used in this study were subjected to multiple passages (> three generations) under standard laboratory conditions to ensure that maternal effects were excluded. *Daphnids* are cultured in a 1 L conical flask in ADaM (Aachener Daphnien Medium) at 25 ± 1°C, a 16 h photoperiod and pH between 7-7.5[5]. The medium was changed weekly to prevent poor medium quality, and the animals were fed once daily with *Chlorella pyrenoidosa* at a final concentration of 3×10^5 algal cells/ml[52] (Supplemental Video 2 and 3). With the exception of the life history observation experiment and the longevity experiment, all experimental *daphnids* in this study were 10-day-old (adults) parthenogenetic individuals without eggs to ensure that the *daphnids* were at the same developmental stage in each experiment. All samples were rinsed 3-4 times with sterile ddH_2O to remove contaminating bacteria and *daphnids* samples for genome sequencing and the LC-MS/MS experiment are placed in clean media a day in advance to empty the bacteria and algae in the gut. All samples were snap frozen in liquid nitrogen and then stored at -80 °C for using.

Medicines and reagents

Sodium dichloroacetate (DCA) (purity > 98%) and octopamine hydrochloride (OA) (purity ≥ 98%) were purchased from Shanghai Yuanye Bio-Technology Co. (Shanghai, China). 6,8-Bis(benzylthio) octanoic acid (CPI-613) (purity > 98%) was purchased from Tokyo Chemical Industry Co., Ltd. All drugs were stored at −20°C, protected

from light, and dissolved in dimethyl sulfoxide (Nanjing Jiancheng Bioengineering Institute, China) before use.

Genome sequencing, assembly, and annotation of the *S. vetulus*

Genomic DNA was extracted using the Qiagen kit (Qiagen, Germany) according to the manufacturer's instructions. Genomic DNA purity (OD260/280 and OD260/230), concentration and integrity were determined using Nanodrop 2000 (Thermo Fisher Scientific, USA), Qubit 3.0 (Invitrogen, USA) and 1% agarose gel electrophoresis (voltage: 100 V, electrophoresis time: 40 min). Sequencing libraries for Illumina NovaSeq and single-molecule real-time sequencing (SMRT) on the PacBio Sequel platform were constructed from qualified DNA samples. Library quality of the library was assessed using Qubit 3.0 and Agilent 2100 (Agilent, USA) to ensure that sequencing requirements were met.

Hi-C sequencing library construction. After formaldehyde crosslinking and fixation of live *S. vetulus* isolates, the crosslinking products were enzymatically cleaved using restriction endonucleases to produce sticky ends. Biotin-labelled nucleotides were then added for end repair to form flat ends, and ligase was used for the flat-end joining reaction to form a molecular loop. Hi-C samples were then prepared by DNA purification and extraction. After passing the test, the end-labelled biotin was removed, cleaved by ultrasound, end repaired, base A added, and sequencing junctions added to form the junction product; then the PCR conditions were screened and amplified to obtain the library product. After passing quality control, the constructed library was sequenced on the Illumina HiSeq platform to provide raw data for subsequent analysis.

The Pacbio sequencing data were corrected, trimmed and assembled using Canu software to assemble the reads into contigs and generate consensus sequences. The raw data were compared to the assembled genome using blasr software, and then the completed bam files were compared using samtools to sort by position and indexed using pbindex. The assembled fasta files were also indexed using samtools, and then the next step of error correction could be performed using arrow. In the three-generation polish with arrow, the number of threads will be set as large as possible to speed up the run, minCoverage is set to 15, the result file of the blasr comparison and the assembled genome are input, and error corrected genome is output. The results obtained will then be genome survey of the second generation of data, through the BWA software will be reads compared to the three generations of Polish after the genome, using pilon software for error correction. The genomes were de-redundant after preliminary assembly and error correction using the software purge haplotigs.

Hi-C-assisted assembly: After the downstream Hi-C raw downstream data were filtered and de-redundant, the resulting Hi-C reads of *S. vetulus* were compared to the whole genome outline by BWA and then processed by samtools to obtain high-quality comparison data. The filtered comparison results were analyzed using Lachesis for clustering, sorting and orientation of super-scaffolds, and finally, genomic overlapping regions were identified based on sequence homology and the highly phasic nature of distant interaction patterns, and scaffolds were merged based on the overlapping regions and anchored to the chromosomes to obtain the final chromosome-level scaffolds. The final chromosome-level scaffolds were obtained using juicer software for evaluation and correction of the assembly results and visualization in the form of heat maps. Genomic circle maps were generated using the Circos software and used to present the assessment results as a whole.

The repetitive sequences of the genome were masked, and then genomic functional annotation and non-coding RNA annotation were performed. The genome with blocked repetitive sequences was used for genomic functional annotation, and all gene sequences were compared with InterPro, GO, KEGG, Swissprot, TrEMBL, TF, Pfam, NR, and KOG protein databases using BLASTX software with the parameter setting E-value of BLASTX software: 1e-5.

Comparative genomics analysis

Fourteen species for which genomic data were available were downloaded from the NCBI database: *Acyrthosiphon pisum*, *Aphis gossypii*, *Myzus persicae*, *Sipha flava*, *Cinara cedri*, *Armadillidium nasatum*, *Eumeta japonica*, *Frankliniella occidentalis*, *Penaeus vannamei*, *and Tigriopus californicus*, coding sequence (CDS) sequences of *D. sinensis*, *D. magna*, *D. pulex*, and *Actinia tenebrosa*. Blast comparison (e-value ≤ 1e-5) of the CDS of 15 species was first performed, and then gene family clustering analysis was performed using OrthoMCL (v.2.0.9) software. Based on the results of the OrthoMCL run, single-copy homologous genes were selected from all the homologous genes to construct the protein sequences of the supergenes, and the sequences of the 15 species were compared using MAFFT (v.7.294). The conserved sites in the multiple sequence alignment results were then extracted using Gblocks software (v.0.91b) software according to the default parameters. *A. tenebrosa* was used as an outgroup to construct a maximum likelihood phylogenetic tree using IQ-TREE (v.1.6.9) with a bootstrap value of 1000. Species divergence time were estimated using MCMCTREE software, and the divergence time pairs were obtained from the TimeTree website (http://www.timetree.org) and the related literature. The divergence times in the literature were used to correct the obtained time correction points. The amplification and contraction analysis of *S. vetulus* gene family was then performed using CAFE software (http://sourceforge.net/projects/cafehahnlab/). The proteins of *S. vetulus* and *D. sinensis* were compared using Blastp (v.2.6.0), and then based on the comparison results, covariance analysis was performed using MCScanX (http://chibba.pgml.uga.edu/mcscan2/) to plot the chromosome covariance scatterplots and circle plots of *S. vetulus* and *D. sinensis*.

Life history observation experiment

A healthy parthenogenetic individual (F_0) with eggs was selected and its offspring were used to study the life history[5]. After being released from the parthenogenetic mother (F_0), more than 10 newborns (F_1) were cultured separately and observed until death. During the experiment, *S. vetulus* were fed with *S. obliquus* every day, the medium was changed every three days, F_2 were removed every day, and the body length and reproduction of the newborns (F_1) were measured and recorded every single day. We then calculated the life span (in days), body length at sexual maturity, age at sexual maturity, time gap between each reproduction (the inter-clutch period), the number of offspring per clutch (brood size) and total number of offspring for each individual (total reproductive capacity). Maturity was considered as the moment at which eggs can be observed in the female's brood pouch for the first time[53]. The rearing conditions were as previous description.

Measurement of several physiological and behavioral parameters

Hopping frequency. Swimming by hopping is a characteristic movement of *daphnids*, caused by rhythmic hopping of the second antennae. The hopping frequency is the total number of hops in a given time period[54].

Swimming trajectory and locomotor activity. The swimming trajectory and locomotor activity of *daphnids* were measured using the method described by Bownik. The swimming behavior of *S. vetulus* and *D. sinensis* in 6-well plates was videotaped for 1 min using a fixed digital video camera. The swimming tracks were analyzed on a frame-by-frame basis using the Tracker® 6.0, and the locomotor activity is expressed as the distance swum per unit of time (mm/min)[55].

Duration of quiescence. the duration of quiescence was used in the study to characterize the specific swimming habits of *S. vetulus*. This period of time when no movement is observed is referred to as quiescence[54]. The movements of the *daphnids* were recorded to count the time of immobility and expressed as the ratio of the time of immobility to the total duration.

Oxygen consumption. The respiration rate of *daphnids* was calculated by measuring dissolved oxygen concentrations assay in the culture medium. Dissolved oxygen measurements were performed using Hach Portable Water Quality Instruments. The initial dissolved oxygen concentration in the medium and the dissolved oxygen concentration after 6 h of sealing were measured and the oxygen consumption rate was calculated (mg O_2 ind.$^{-1}$ h^{-1}).

Feeding rate. Algae were sampled from each well of a six-well plate at 4 and 10 h after feeding[55]. Algal densities were determined directly using a light microscope (Nikon BM2000) at × 400 magnification. The feeding rate (I, cells animal individuals^{-1} h^{-1}, i.e., clearance rate) was calculated as the difference in algal densities between the beginning and the end of the experimental wells according to the following equations, which are commonly used in plankton:

$$\mathrm{FR} = \frac{\mathrm{V}\left[\ln(C_0 - \Delta C_b) - \ln(C_1 - \Delta C_b)\right]}{\mathrm{Nt}}$$

$$I = \frac{FR(C_0 + C_1)}{2}$$

Where FR is the filter rate (mL/ind./h); V is the volume of the culture (mL); C_0 and C_1 are the algal density at the beginning and the end of the experimental wells (cells/mL), respectively; ΔC_b is the difference in algal density in the blank wells (no grazers) at 6 hours; N is the number of *daphnids* and t is the duration of the experiment (h); I is the feeding rate (cells/ind./h).

Heart rate and thoracic limb activity. The number of heartbeats per minute is defined as the heart rate of *D. sinensis*. The number of oscillations of thoracic limb per minute is defined as thoracic limb activity of *daphnids*. Each water flea individual was recorded for at least 2 min using a digital microscope (DMS-2020A, MPI) with video recording and imaging capabilities. Video editing software (Adobe premiere pro 2020) was used to slow down the video by a factor of 0.2 to facilitate the counting of thoracic limb activity and the heart rate.

LC-MS/MS data acquisition and analysis

Sample collection: *S. vetulus* and *D. sinensis* of the same age (10 days) and feeding environment were selected for metabolomics analysis. Every 200 *daphnids* were considered as one sample, and three technical replicates were set up for *S. vetulus* and *D. sinensis*, respectively, for a total of six samples. Quality control was performed in this experiment, and the researchers also prepared QC samples, which were aliquots of all the samples mixed together. QC samples were used to equilibrate the chromatography-mass spectrometry (CS-MS) system and to determine the status of the instrument, and were used for the evaluation of the system's stability throughout the experiment.

Sample pre-treatment: Metabolites were extracted from homogenized samples with 1 ml 70% methanol. Samples were first vortexed for 5 min and placed on ice for 15 min. The samples were then centrifuged at 13523 × g for 10 min at 4 °C and 400 µL of the supernatant was stored overnight at -20°C. Finally, the samples were centrifuged at 13523 × g for 3 min at 4 °C and 200 µL of supernatant was used for metabolite detection.

The instrumentation for data acquisition consisted mainly of ultra-performance liquid chromatography (UPLC) (ExionLC AD, AB Sciex, Framingham, MA, USA) and tandem mass spectrometry (MS/MS, QTRAP5500, AB Sciex, Framingham, MA, USA).

Mainly liquid phase conditions: (1) Column: Waters ACQUITY UPLC HSS T3 C18 1.8 µm, 2.1 mm*100 mm; (2) mobile phase: ultrapure water (0.1% formic acid) in phase A, and acetonitrile (0.1% formic acid) in phase B. The mobile phase was 0.1% formic acid (0.1% formic acid); (3) elution gradient: 0 min water/acetonitrile (95:5 V/V), 10.0 min 10:90 V/V, 11.0 min 10:90 V/V, 11.1 min 95:5 V/V, 14.0 min 95:5 V/V. The elution rate was 0.4 ml/kg; (4) flow rate of 0.4 ml/min; column temperature of 40 °C; injection volume of 2 µL.

The mass spectrometry conditions mainly included: Electrospray ionization (ESI) temperature 500 °C, mass spectrometry voltage 5500 V (positive), -4500 V (negative), ionization gas I (GS I) 55 psi, gas II (GS II) 60 psi, curtain gas (CUR) 25 psi, and the collision-activated dissociation (CAD) parameter was set to high. In a triple quadrupole (Qtrap), each ion pair was detected by scanning based on optimized declustering potential (DP) and collision energy (CE)[56].

Data processing and quantification: Chromatographic peak areas and retention times were extracted using MultiQuant 3.0.2. Retention times were corrected using energy metabolite standards for metabolite identification[57]. Ion peak areas of metabolites were normalized by internal standards L-Glutamate-d5 and Succinate-d6. Standard curves were plotted based on the intensity values of the standards. The upsampling concentrations of metabolites were calculated using the standard curve. The concentration of metabolites in the sample was calculated by substitution according to the pretreatment treatment (Supplementary Data 1).

Amino acid sequence comparison and prediction of protein-ligand interactions

Multiple Sequence Alignment in DNAMAN (version 9.0) was used for amino acid sequence alignment. Access the AlphaFold Server via a web browser, upload sequence data including the respective PDH protein sequences of *D. sinensis* and *S. vetulus* and their ligand TPP, and select the corresponding sequence input format[38]. After completing the data upload, the prediction results were viewed, and the 3D protein structures were visualized using PyMOL (Version 3.1.3.). Based on the results provided by AF3, the interactions between the respective PDH proteins of *D. sinensis* and *S. vetulus* and TPP were analyzed, including the predicted protein structures with docking scores (Fig. 1b). Here, we assessed the quality of the predicted protein-ligand interactions using the ranking score, which is a composite metric including pLDDT, PAE, fraction disordered, and has_clash values calculated as 0.8 × ipTM + 0.2 × pTM + 0.5 × disorder − 100 × has_clash.

Pyruvate dehydrogenase (PDH) activity assay

The PDH Activity Assay Kit (Beijing Solarbio Science & Technology Co., Ltd) was used to quantify PDH activity in *daphnids*. Three replicates of 100 *daphnids* per treatment were collected 24 hours after treatment, washed three times in ultrapure water, and frozen at −80 °C. *Daphnids* were homogenized in an ice bath according to the manufacturer's instructions, and the supernatant was centrifuged at 11,000 g for 10 min at 4 °C. 10 µL of supernatant and 180 µL of the working solution were added to the assay plate, and the OD value at 605 nm was determined. The same supernatant used to measure the total protein concentration using a BCA protein assay kit (Jiancheng, Nanjing, China). ATP levels were normalized to the protein content.

Forced exercise experiments

Based on observations of the perching and locomotion habits of *S. vetulus*, there are two main conditions under which *S. vetulus* remains stationary: i. climbing on the surface of aquatic grasses or other substrates in water and, under laboratory conditions, on the walls of culture vessels. Second, use the tension of the water surface when

suspended in water. The forced exercise experiment was designed according to these two points. A clean and smooth glass petri dish was chosen as the experimental vessel so that *S. vetulus* could not climb to the surface of the vessel. The petri dishes containing *S. vetulus* and *D. sinensis* were placed on a shaker and shaken slowly at a frequency of 40 Hz at a constant speed to disturb the water column so that the aged low-fronted grebes could not use the water surface tension to stay still on the water surface. The movements of *S. vetulus* and *D. sinensis* were then observed and recorded hourly by counting the number of *daphnids* individuals that remained suspended and swam and the number of *daphnids* sinking at each time point. Samples of *S. vetulus* and *D. sinensis* were collected after 6 hours of forced exercise, and ATP content and lactate level were examined in *S. vetulus* and *D. sinensis* before and after exercise.

Pdhα Knockout by CRISPR/Cas9

The *pdhα* knockout lines of *D. sinensis* were generated using CRISPR/Cas9[58]. The cDNA and DNA sequences of *pdhα* were identified from the *D. sinensis* genome in our laboratory, with clear delineation of exon and intron regions. Utilizing the CRISPRscan online platform, target sequences within the *pdhα* DNA sequence were identified. The OligoEvaluator online tool was then employed to assess the quality of these target sequences. The local BLAST component of NCBI (National Center for Biotechnology Information) was employed to confirm that the target sequences correspond to a unique locus within the *D. sinensis* genome, thereby finalizing the target sequences for subsequent use. The gRNA for the *pdhα* knockout lines of *D. sinensis* was synthesized using the GeneArt™ Precision gRNA Synthesis Kit (Invitrogen, USA), following the manufacturer's protocol. The obtained gRNA product, after being quantified for concentration, was diluted to a working solution of 1000 ng/μL and aliquoted for storage at -80°C. More details of the experiment are in the Supplementary Material.

Before the injection procedure, the components (Table 1), including TrueCut™ Cas9 Protein v2 at a concentration of 5000 ng/μL (Thermo Fisher Scientific Inc., USA), were mixed and then introduced into capillary glass needles prepared using the NARISHIGE PC−100 programmable vertical micromanipulator (Micrology (Wuhan) Precision Insuments, Ltd.). Using the two-stage pull method (NO. 1/NO. 2 heater level: 80°C/75°C; weight: 2 type light and 0 type heavy), one glass capillary (G−1) is pulled on the Micropipette Puller (PC−100) for capillary pulling operation, carefully remove and mirror check the pulled capillary (Supplemental Video 4). Then fix the capillary at an inclination of 30 in the groove of the Micropipette Grinder (KDG-01), rotate the knob so that capillary slowly down. Start the timer when the tip of the capillary coincides with its shadow, after about 10 s carefully remove and mirror check, if the capillary fails to open successfully, repeat the above operation until you get the capillary tip as seen in the video. The above instruments were purchased from Micrology (Wuhan) Precision Induments, Ltd. Microinjection was performed using Digital Pneumatic Microinjection Pump (DMP-300, Micrology (Wuhan) Precision Insuments, Ltd.).

After the embryos had developed for 30 hours post-injection, genomic DNA from the injected embryos is extracted. Subsequently, the target gene DNA segment, which includes the target site, was amplified using PCR. Agarose gel electrophoresis was then employed to detect any mutations in the targeted region. Table 2 delineates the *pdhα* gRNA targets and their corresponding primers employed in this research.

Table 1 | Reagent Ratios

Reagent	Volume
pdhα gRNA (1000 ng/μL)	1 μL
TrueCut™ Cas 9 Protein (5000 ng/μL)	1 μL
Phenol Red	0.5 μL
DNase/RNase-Free Water	2.5 μL
Total	5 μL

Detection of ATP content and lactate levels

All experimental *daphnids* for the measurement of ATP content and lactate level were 10-day-old parthenogenetic individuals (adult individuals) without eggs. The ATP assay kit from Beyotime Biotechnology was used to measure ATP levels. *Daphnids* were treated with different drug concentrations or DMSO (control) in triplicate for 24 hours. Following the manufacturer's instructions, the samples were homogenized and centrifuged at 4°C for 5 min at 12,000 g. The supernatant was mixed with the assay working solution, and luminescence was measured using a SpectraMax i3x Multi-Mode Microplate Reader (Molecular Devices). ATP levels were normalized to protein levels.

Lactate assay kits (Nanjing Jiancheng Bioengineering Institute, China.) and β-hydroxybutyrate and acetylacetone assay kits (Beijing Solarbio Science & Technology Co., Ltd.) were used to determine lactate and β-hydroxybutyrate and acetylacetone levels. The samples were homogenized and centrifuged according to the manufacturer's instructions to obtain the supernatant. The supernatants were mixed with the appropriate working reagents. The absorbance of lactate was measured at 530 nm and that of β-hydroxybutyrate and acetylacetone were measured at 340 nm.

Assay of octopamine levels

Octopamine levels were quantified using a one-step double antibody sandwich enzyme-linked immunosorbent assay (Octopamine ELISA Assay Kit, Abmart (Shanghai) Co., Ltd.) in *daphnids*. Octopamine antibody-coated wells were sequentially coated with sample, standard, and HRP-labeled detection antibodies. The wells were then washed thoroughly and incubated at a constant temperature. The color was generated using TMB as the substrate, which was catalyzed to blue by peroxidase and later converted to the final yellow color by the addition of acid. Absorbance at 450 nm was measured using a SpectraMax i3x Multi-Mode Microplate Reader (Molecular Devices). In addition, the protein concentration in the samples was simultaneously determined using the BCA Protein Assay Kit (Jiancheng, Nanjing, China), and octopamine levels were normalized to protein levels.

Lifespan Analysis

Healthy female *daphnids* with eggs from the same batch were carefully selected and newly hatched juveniles were collected for lifespan

Table 2 | The *pdhα* gRNA targets and their corresponding primers

For genotypin /qPCR analysis	Forward primer (5′ - 3′)	Reverse primer (5′ - 3′)
pdhα-48	TAATACGACTCACTATAGGCTGCTTTGAAGGAAC	TTCTAGCTCTAAAACATCGGTTCCTTCAAAGCAG
pdhα-64	TAATACGACTCACTATAGAGCGGCCGGTAATTTA	TTCTAGCTCTAAAACTGTATAAATTACCGGCCGC
pdhα-76	TAATACGACTCACTATAGGAACTTGTCCCGAATA	TTCTAGCTCTAAAACCCTTTATTCGGGACAAGTT
pdhα-T48-10	GCCCAACAACCTTTGGGTG	CGTAGAGCTGGCCTTGATTGG
pdhα-T64-2	CAGCCCTTCAAACTGCACAA	AATCTAACGAACTTGTCCCGA
pdhα-T76-4	TCATCGAGGCTCTCATACCGA	GAAGGATGGAAACAGCGGC

analysis. The juveniles were reared under standardized conditions in a sterile and constant temperature incubator (GZX-400BSH-III, CIMO, Shanghai, China) with appropriate lighting, and survival rates were recorded daily. At 3 days of age, the drug was added to the sterilized medium. An equivalent concentration of DMSO, the drug solvent, was added to the culture medium of pups in the control group. To ensure the effective concentration of the drug, the culture media were changed every other day.

Statistical Analysis

Data were analyzed and visualized using GraphPad Prism 8.02. Results are expressed as the mean ± SEM. The Shapiro-Wilk test was used to test for normal distribution. Unpaired two-tailed Student's t-test, one-way ANOVA and Tukey's multiple range test, two-way ANOVA with Sidak's multiple-comparisons, two-way ANOVA with Dunnett's multiple-comparisons test and Survival curve comparison with Gehan-Breslow-Wilcoxon test were used to assess the significance of differences between groups.

Reporting summary

Further information on research design is available in the Nature Portfolio Reporting Summary linked to this article.

Data availability

The genome information generated in this study has been deposited in the NCBI's GenBank database under accession code GCA_041003635.1 [https://www.ncbi.nlm.nih.gov/datasets/genome/GCA_041003635.1/]. Metabolomics raw data have been uploaded to the OMIX database of China National Center for Bioinformation (CNCB), OMIX ID: OMIX009479. Source data are provided with this paper.

References

1. Dudycha, J. L. & Hassel, C. Aging in sexual and obligately asexual clones of Daphnia from temporary ponds. *J. Plankton Res.* **35**, 253–259 (2013).
2. Constantinou, J., Sullivan, J. & Mirbahai, L. Ageing differently: Sex-dependent ageing rates in Daphnia magna. *Exp. Gerontol.* **121**, 33–45 (2019).
3. Ukhueduan, B., Schumpert, C., Kim, E., Dudycha, J. L. & Patel, R. C. Relationship between oxidative stress and lifespan in Daphnia pulex. *Sci. Rep.* **12**, 2354 (2022).
4. King, K. C., Hall, M. D. & Wolinska, J. Infectious disease ecology and evolution in a changing world. *Philos. Trans. R. Soc. B Biol. Sci.* **378**, 20220002 (2023).
5. Jia, J. et al. Multi-omics perspective on studying reproductive biology in Daphnia sinensis. *Genomics* **114**, 110309 (2022).
6. Speakman, J. R. & Selman, C. Physical activity and resting metabolic rate. *Proc. Nutr. Soc.* **62**, 621–634 (2003).
7. Van Voorhies, W. A. & Ward, S. Genetic and environmental conditions that increase longevity in *Caenorhabditis elegans* decrease metabolic rate. *Proc. Natl Acad. Sci.* **96**, 11399–11403 (1999).
8. Kassi, E. & Papavassiliou, A. G. Could glucose be a proaging factor? *J. Cell. Mol. Med.* **12**, 1194–1198 (2008).
9. Pessoa, J. Shifting metabolism to increase lifespan. *Trends Endocrinol. Metab.* **33**, 533–535 (2022).
10. Lee, S. S. et al. A systematic RNAi screen identifies a critical role for mitochondria in C. elegans longevity. *Nat. Genet.* **33**, 40–48 (2002).
11. Hansen, M., Hsu, A.-L., Dillin, A. & Kenyon, C. New Genes Tied to Endocrine, Metabolic, and Dietary Regulation of Lifespan from a Caenorhabditis elegans Genomic RNAi Screen. *PLoS Genet.* **1**, e17 (2005).
12. Lin, S.-J. et al. Calorie restriction extends Saccharomyces cerevisiae lifespan by increasing respiration. *Nature* **418**, 344–348 (2002).
13. Hipkiss, A. R. On the mechanisms of ageing suppression by dietary restriction—is persistent glycolysis the problem? *Mech. Ageing Dev.* **127**, 8–15 (2006).
14. Lin, S.-J. et al. lifespan by increasing respiration. (2002).
15. Lionaki, E. et al. Mitochondrial protein import determines lifespan through metabolic reprogramming and de novo serine biosynthesis. *Nat. Commun.* **13**, 651 (2022).
16. Lee, S.-J., Hwang, A. B. & Kenyon, C. Inhibition of Respiration Extends C. elegans Life Span via Reactive Oxygen Species that Increase HIF-1 Activity. *Curr. Biol.* **20**, 2131–2136 (2010).
17. Yap, K. N. et al. Naked mole-rat and Damaraland mole-rat exhibit lower respiration in mitochondria, cellular and organismal levels. *Biochim. Biophys. Acta BBA - Bioenerg.* **1863**, 148582 (2022).
18. Yuan, R., Hascup, E., Hascup, K. & Bartke, A. Relationships among Development, Growth, Body Size, Reproduction, Aging, and Longevity – Trade-Offs and Pace-Of-Life. *Biochem. Mosc.* **88**, 1692–1703 (2023).
19. Gray, L. R., Tompkins, S. C. & Taylor, E. B. Regulation of pyruvate metabolism and human disease. *Cell. Mol. Life Sci.* **71**, 2577–2604 (2013).
20. Zhao, X. et al. DCA Protects against Oxidation Injury Attributed to Cerebral Ischemia-Reperfusion by Regulating Glycolysis through PDK2-PDH-Nrf2 Axis. *Oxid. Med. Cell. Longev.* **2021**, 5173035 (2021).
21. Schoenmann, N., Tannenbaum, N., Hodgeman, R. M. & Raju, R. P. Regulating mitochondrial metabolism by targeting pyruvate dehydrogenase with dichloroacetate, a metabolic messenger. *Biochim. Biophys. Acta BBA - Mol. Basis Dis.* **1869**, 166769 (2023).
22. Vasan, K., Werner, M. & Chandel, N. S. Mitochondrial Metabolism as a Target for Cancer Therapy. *Cell Metab.* **32**, 341–352 (2020).
23. Maciak, S. & Konarzewski, M. Repeatability of standard metabolic rate (SMR) in a small fish, the spined loach (Cobitis taenia). *Comp. Biochem. Physiol. A. Mol. Integr. Physiol.* **157**, 136–141 (2010).
24. Chabot, D., Steffensen, J. F. & Farrell, A. P. The determination of standard metabolic rate in fishes. *J. Fish. Biol.* **88**, 81–121 (2016).
25. Cai, M. et al. Changes in ultrastructure of gonads and external morphology during aging in the parthenogenetic cladoceran Daphnia pulex. *Micron* **122**, 1–7 (2019).
26. Roeder, T. The control of metabolic traits by octopamine and tyramine in invertebrates. *J. Exp. Biol.* **223**, jeb194282 (2020).
27. Li, Y. et al. Octopamine controls starvation resistance, life span and metabolic traits in Drosophila. *Sci. Rep.* **6**, 35359 (2016).
28. Pietrzak, B., Grzesiuk, M., Dorosz, J. & Mikulski, A. When males outlive females: Sex-specific effects of temperature on lifespan in a cyclic parthenogen. *Ecol. Evol.* **8**, 9880–9888 (2018).
29. Sin, T. K., Yung, B. Y. & Siu, P. M. Modulation of SIRT1-Foxo1 Signaling axis by Resveratrol: Implications in Skeletal Muscle Aging and Insulin Resistance. *Cell. Physiol. Biochem.* **35**, 541–552 (2015).
30. Mayers, R. M., Leighton, B. & Kilgour, E. PDH kinase inhibitors: a novel therapy for Type II diabetes? *Biochem. Soc. Trans.* **33**, 367–370 (2005).
31. Yao, Y. et al. Pyruvate dehydrogenase kinase 1 protects against neuronal injury and memory loss in mouse models of diabetes. *Cell Death Dis.* **14**, 722 (2023).
32. Yonashiro, R., Eguchi, K., Wake, M., Takeda, N. & Nakayama, K. Pyruvate Dehydrogenase PDH-E1β Controls Tumor Progression by Altering the Metabolic Status of Cancer Cells. *Cancer Res.* **78**, 1592–1603 (2018).
33. Stacpoole, P. W. The pyruvate dehydrogenase complex: Life's essential, vulnerable and druggable energy homeostat. *Mitochondrion* **70**, 59–102 (2023).
34. Patel, K. P., O'Brien, T. W., Subramony, S. H., Shuster, J. & Stacpoole, P. W. The spectrum of pyruvate dehydrogenase complex

deficiency: Clinical, biochemical and genetic features in 371 patients. *Mol. Genet. Metab.* **105**, 34–43 (2012).
35. Pedersen, S., Bliksrud, Y. T., Selmer, K. K. & Ramm-Pettersen, A. Pyruvatdehydrogenase-mangel. *Tidsskr. Den Nor. Legeforening* https://doi.org/10.4045/tidsskr.18.0988 (2019).
36. *Macromolecular Protein Complexes*. vol. 83 (Springer International Publishing, Cham, 2017).
37. Imbard, A. et al. Molecular characterization of 82 patients with pyruvate dehydrogenase complex deficiency. Structural implications of novel amino acid substitutions in E1 protein. *Mol. Genet. Metab.* **104**, 507–516 (2011).
38. Abramson, J. et al. Accurate structure prediction of biomolecular interactions with AlphaFold 3. *Nature* **630**, 493–500 (2024).
39. Ng, J. C. M. & Schooling, C. M. Effect of basal metabolic rate on lifespan: a sex-specific Mendelian randomization study. *Sci. Rep.* **13**, 7761 (2023).
40. Abbott, A. Reduced-calorie diet shows signs of slowing ageing. *Nature* **555**, 570–571 (2018).
41. Duarte, L. C. & Speakman, J. R. Low resting metabolic rate is associated with greater lifespan because of a confounding effect of body fatness. *AGE* **36**, 9731 (2014).
42. Zhang, L., Yang, F. & Zhu, W.-L. Evidence for the 'rate-of-living' hypothesis between mammals and lizards, but not in birds, with field metabolic rate. *Comp. Biochem. Physiol. A. Mol. Integr. Physiol.* **253**, 110867 (2021).
43. Schulz, T. J. et al. Glucose Restriction Extends Caenorhabditis elegans Life Span by Inducing Mitochondrial Respiration and Increasing Oxidative Stress. *Cell Metab.* **6**, 280–293 (2007).
44. Belhadj Slimen, I. et al. Reactive oxygen species, heat stress and oxidative-induced mitochondrial damage. A review. *Int. J. Hyperth.* **30**, 513–523 (2014).
45. Van Breugel, F., Suver, M. P. & Dickinson, M. H. Octopaminergic modulation of the visual flight speed regulator of *Drosophila*. *J. Exp. Biol.* jeb.098665 https://doi.org/10.1242/jeb.098665 (2014).
46. Noble, T., Stieglitz, J. & Srinivasan, S. An Integrated Serotonin and Octopamine Neuronal Circuit Directs the Release of an Endocrine Signal to Control C. elegans Body Fat. *Cell Metab.* **18**, 672–684 (2013).
47. Wang, M., Wang, Q. & Whim, M. D. Fasting induces a form of autonomic synaptic plasticity that prevents hypoglycemia. *Proc. Natl. Acad. Sci.* **113**, E3029–E3038 (2016).
48. Schulte, P. M. The effects of temperature on aerobic metabolism: towards a mechanistic understanding of the responses of ectotherms to a changing environment. *J. Exp. Biol.* **218**, 1856–1866 (2015).
49. Kim, B., Lee, J., Kim, Y. & Lee, S.-J. V. Regulatory systems that mediate the effects of temperature on the lifespan of *Caenorhabditis elegans*. *J. Neurogenet.* **34**, 518–526 (2020).
50. Cornelissen, V. A., Verheyden, B., Aubert, A. E. & Fagard, R. H. Effects of aerobic training intensity on resting, exercise and post-exercise blood pressure, heart rate and heart-rate variability. *J. Hum. Hypertens.* **24**, 175–182 (2009).
51. Gaye, B. et al. Association between change in heart rate over years and life span in the Paris Prospective 1, the Whitehall 1, and Framingham studies. *Sci. Rep.* **14**, 20052 (2024).
52. Qi, H. et al. Cloning and functional analysis of the molting gene CYP302A1 of Daphnia sinensis. *Front. Zool.* **20**, 2 (2023).
53. Richard, R., Zhang, Y.-K. & Hung, K.-W. Thermal dependence of Daphnia life history reveals asymmetries between key vital rates. *J. Therm. Biol.* **115**, 103653 (2023).
54. Tkaczyk, A., Bownik, A., Dudka, J., Kowal, K. & Ślaska, B. Daphnia magna model in the toxicity assessment of pharmaceuticals: A review. *Sci. Total Environ.* **763**, 143038 (2021).
55. Bownik, A. Daphnia swimming behaviour as a biomarker in toxicity assessment: A review. *Sci. Total Environ.* **601–602**, 194–205 (2017).
56. Chen, W. et al. A Novel Integrated Method for Large-Scale Detection, Identification, and Quantification of Widely Targeted Metabolites: Application in the Study of Rice Metabolomics. *Mol. Plant* **6**, 1769–1780 (2013).
57. Fraga, C. G., Clowers, B. H., Moore, R. J. & Zink, E. M. Signature-Discovery Approach for Sample Matching of a Nerve-Agent Precursor Using Liquid Chromatography–Mass Spectrometry, XCMS, and Chemometrics. *Anal. Chem.* **82**, 4165–4173 (2010).
58. Mali, P. et al. RNA-Guided Human Genome Engineering via Cas9. *Science* **339**, 823–826 (2013).

Acknowledgements

This article was supported by National Natural Science Foundation of China (32471583 and 32071516 for X.J.L.) and Finance Special Fund of Chinese Ministry of Agriculture and Rural Affairs of the People's Republic of China for X.J.L.(Fisheries resources and environment survey in the key water areas of Southwest China).

Author contributions

G.H., W.C. and X.L. conceived the research and designed the experiments. W.C. carried out the experiments. X.X. M.Z. and Z.Z. prepared the samples and analyzed the data. W.C. wrote the manuscript with input from the other authors. J.C. and A.S. examined and polished the manuscript. G.H., D.L. and X.J. supervised the research. All authors contributed to the interpretation and drafting of the paper.

Competing interests

The authors declare no competing interests.

Additional information

Supplementary information The online version contains supplementary material available at https://doi.org/10.1038/s41467-025-58666-w.

Correspondence and requests for materials should be addressed to Liu Xiangjiang.

Peer review information *Nature Communications* thanks Charles V Mobbs and the other, anonymous, reviewer(s) for their contribution to the peer review of this work. A peer review file is available.